Robust Functional Connectivity from MEG using Network Localized Granger Causality: Directional Connectivity Results in Physiological Frequency Bands

Behrad Soleimani[1,2], Proloy Das[3], I.M. Dushyanthi Karunathilake[1,2], Stefanie E. Kuchinsky[4], Jonathan Z. Simon[1,2,5], Behtash Babadi[1,2]

[1]Department of Electrical and Computer Engineering, University of Maryland, College Park, MD, [2]Institute for Systems Research, University of Maryland, College Park, MD, [3]Department of Anesthesia, Critical Care and Pain Medicine, Massachusetts General Hospital, Boston, MA, USA, [4]Audiology and Speech Pathology Center, Walter Reed National Military Medical Center, Bethesda, MD, USA, [5]Department of Biology, University of Maryland College Park, MD, USA

Introduction

- Identifying causal relationships between different cortical areas to understand mechanisms behind sensory processing
- Connectivity characterized by the temporal predictability of activity across brain regions via Granger causality (GC)
- Challenges with Magnetoencephalography (MEG): data are low-dimensional, noisy, and linearly mixed versions of underlying source activities
- Conventional methods (two-stages):

- Drawbacks: bias propagation, especially in spatial leakage

- Goal: *directly* localize GC influences without an intermediate source localization step
- Method: Network Localized Granger Causality (NLGC)

Fig. 1. Schematic of NLGC inference. Bypassing intermediate source localization, cortical connectivity is obtained directly from the MEG observations.

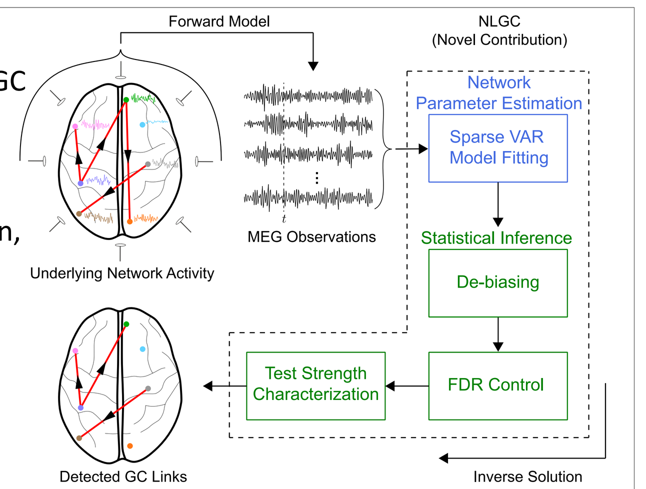

Model

- Observation model:

$$\mathbf{y}_t = \mathbf{C}\mathbf{x}_t + \mathbf{n}_t, \quad t = 1, 2, \cdots, T$$

$\mathbf{y}_t \in \mathbb{R}^M$ MEG observation, $\mathbf{C} \in \mathbb{R}^{M \times N}$ lead field matrix
$\mathbf{x}_t \in \mathbb{R}^N$ source activity, $\mathbf{n}_t \in \mathbb{R}^M$ measurement noise

- Source dynamic model (auto-regressive):

$$\mathbf{x}_t = \sum_{k=1}^{q} \mathbf{A}_k \mathbf{x}_{t-k} + \mathbf{w}_t, \quad t = 1, 2, \cdots, T$$

$\mathbf{A}_k \in \mathbb{R}^{N \times N}$ coefficient matrix, $\mathbf{w}_t \in \mathbb{R}^N$ noise process

- Distributional assumptions:
  - $\mathbf{n}_t \sim$ zero-mean Gaussian (known covariance)
  - $\mathbf{w}_t \sim$ zero-mean Gaussian, independent sources (unknown diagonal covariance $\mathbf{Q}$)

Granger Causality

- Consider link $(\tilde{i} \rightarrow i)$ with following models:

Full: $\mathbf{x}_t^{(i)} = \sum_{j}\sum_{k} a_{i,j,k}\mathbf{x}_{t-k}^{(j)} + \mathbf{w}_t^{(i)}, \quad \mathbf{w}_t^{(i)} \sim \mathcal{N}(0, \sigma_i^2)$

Reduced: $\mathbf{x}_t^{(i)} = \sum_{j \neq \tilde{i}}\sum_{k} a'_{i,j,k}\mathbf{x}_{t-k}^{(j)} + \mathbf{w'}_t^{(i)}, \quad \mathbf{w'}_t^{(i)} \sim \mathcal{N}(0, \sigma_{i\setminus\tilde{i}}^2)$

- Granger Causality (GC) measure:

$$\mathcal{F}_{(\tilde{i} \mapsto i)} = \log\left(\frac{\sigma_{i\setminus\tilde{i}}^2}{\sigma_i^2}\right)$$

relative predictive variance explained

- $\mathcal{F}_{(\tilde{i} \mapsto i)} \gg 0$: GC link exists.

Fig. 2. GC link $(\tilde{i} \rightarrow i)$ implies temporal predictability of source i by $\tilde{i}$.

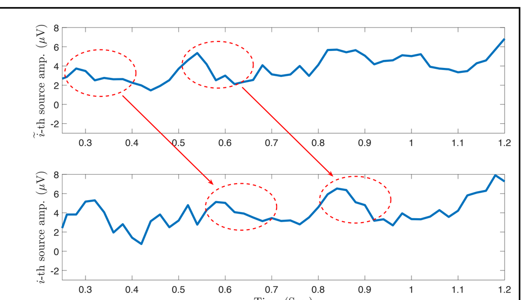

Parameter Estimation†

- Challenge: source activities are unknown
- Solution: Expectation Maximization (EM)
- At the l-th iteration:

$$\text{E-step}: \; Q(\boldsymbol{\theta}|\widehat{\boldsymbol{\theta}}^{(l)}) = \mathrm{E}\left[\log p(\mathbf{x}_{1:T}, \mathbf{y}_{1:T}; \boldsymbol{\theta}) \middle| \mathbf{y}_{1:T}; \widehat{\boldsymbol{\theta}}^{(l)}\right]$$

$$\text{M-step}: \; \widehat{\boldsymbol{\theta}}^{(l+1)} = \underset{\boldsymbol{\theta}}{\operatorname{argmax}} \left\{Q(\boldsymbol{\theta}|\widehat{\boldsymbol{\theta}}^{(l)}) + R_{\ell_1}(\boldsymbol{\lambda}, \boldsymbol{\theta})\right\}$$

- ℓ_1-norm regularization is utilized at the M-step to mitigate the ill-posedness resulting from the low-dimensional measurements

Statistical Inference†

- Two hypothesis for link $(\tilde{i} \rightarrow i)$:
  - $H_{(\tilde{i} \mapsto i),0}$: there is no GC influence
  - $H_{(\tilde{i} \mapsto i),1}$: there is a GC influence
- Asymptotic distributions:

$$[\mathcal{D}_{(\tilde{i} \mapsto i)} | H_{(\tilde{i} \mapsto i),0}] \xrightarrow{d} \chi^2(q)$$

$$[\mathcal{D}_{(\tilde{i} \mapsto i)} | H_{(\tilde{i} \mapsto i),1}] \xrightarrow{d} \chi^2(q, \nu_{(\tilde{i} \mapsto i)})$$

- False discovery rate (FDR) control:
  - Reject null hypothesis at a confidence level α
  - Control FDR via BY procedure

†For more details, please see Soleimani et al. (2022).

Results: Synthetic Data†

Simulation results suggest that NLGC is more reliable compared to the two-stage procedures.

Fig. 3. Comparison of NLGC with two-stage procedures in realistic simulation. **A.** Ground truth GC network example, with estimates from by NLGC and two-stage approaches (using MNE, dSPM, and Champagne) [dorsal & lateral brain plots]. NLGC captures nearly all existing GC links with no spurious detection. **B.** ROC curves (hit rate vs. false alarm) for NLGC and two-stage approaches for exact/relaxed link localization and without/with model mismatch. NLGC has equal (or better) hit rate with low false alarm rate. **C.** SNR effects without/with model mismatch. NLGC consistently maintains low false alarm rates across SNRs.

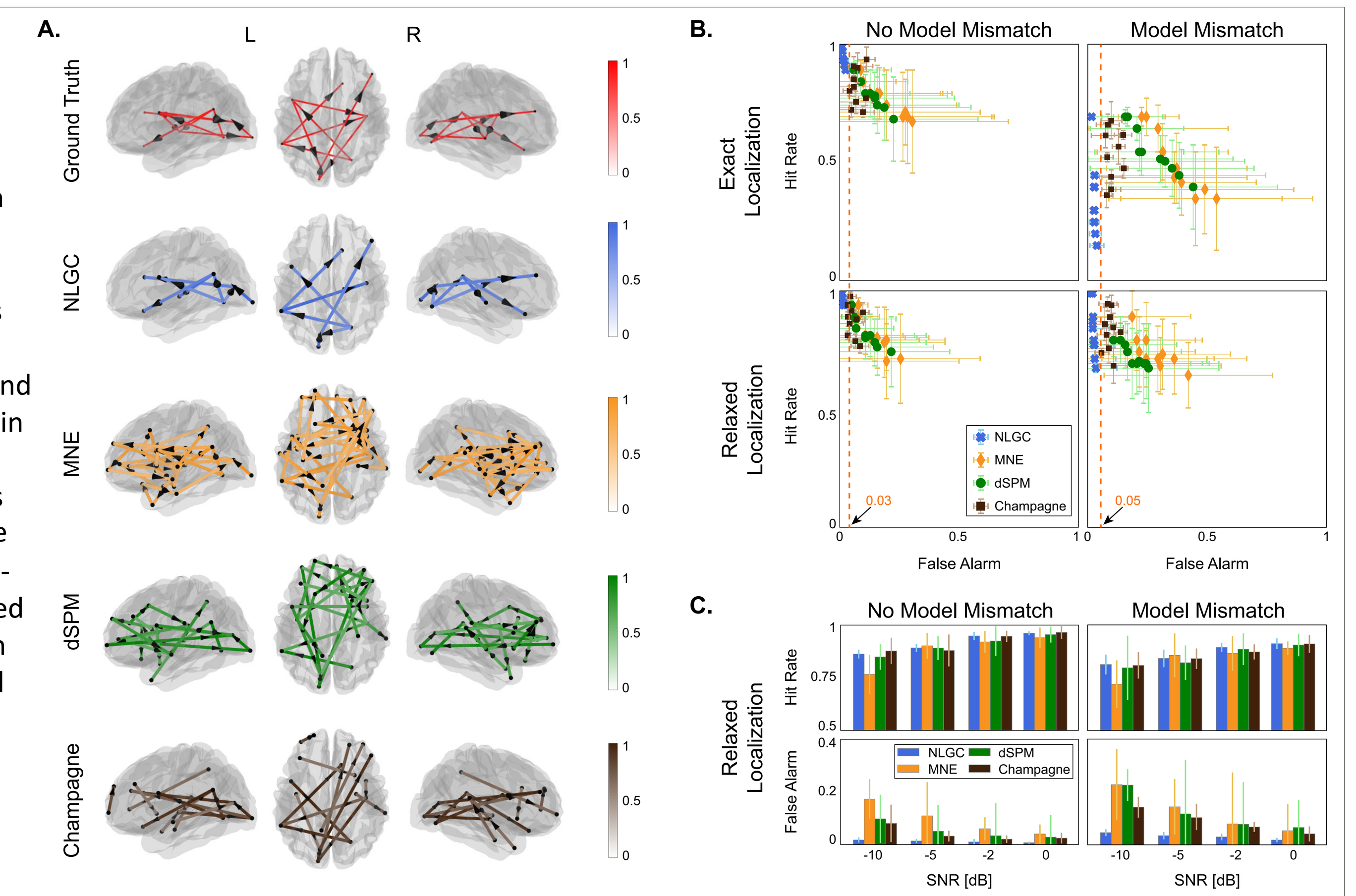

Results: Tone Processing vs. Resting State†

- 13 younger and 9 older adults
- 100 repetitions of tone pips presented at the end of resting state recordings
- Two 40 seconds trials per subject/condition
- Connectivity in auditory cortex is investigated

NLGC identifies network-level age- and condition-related changes in the auditory cortex.

Fig. 4. NLGC analysis of recorded MEG data in two frequency bands. **A.** Extracted GC links between frontal and temporal areas overlaid on dorsal brain plots for younger (top) and older (bottom) adults [0.1-8 Hz]. Notable increase of top-down links from frontal to temporal areas during tone processing compared to resting state. **B.** Percent-age of causal links, averaged over subjects within age-group, between frontal, temporal, and parietal areas for tone processing vs. resting state conditions and younger vs. older adults [0.1-8 Hz]. Dashed ovals indicate indicate corresponding links in **A**. Notable changes across tasks, including dominantly top-down frontal to temporal/parietal connections during tone processing, contrasting with dominant-ly bottom-up temporal/parietal to frontal connections during resting state. **C.** Extracted GC links between frontal and parietal areas overlaid on dorsal brain plots for younger and older adults [13-25 Hz]. Notable increase of frontal to parietal links in tone processing for older adults. **D.** Averaged percentage of causal links between frontal, temporal, and parietal areas for tone processing vs. resting state conditions and younger vs. older adults. Dashed ovals indicate corresponding links in **C**. Notable changes across both tasks and age groups, including higher involvement of parietal areas during resting state, increase of frontal-to-frontal connections for younger participants, and top-down links from frontal to parietal areas for older participants, during tone processing.

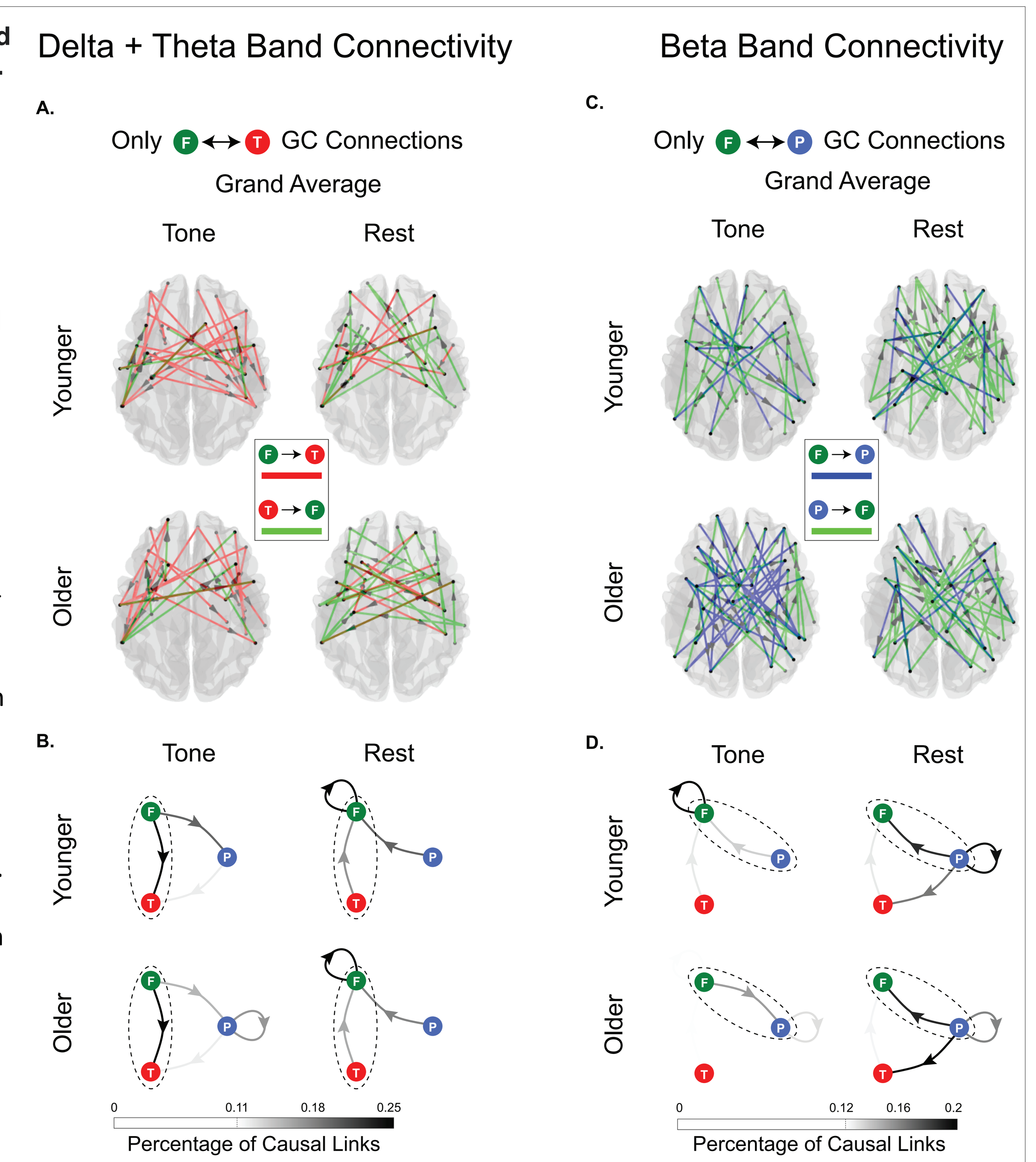

Results: Difficult Listening Experiment

- 1-minute-long speech segments from an audio book in two conditions:
  1) Clean speech (*easy*)
  2) Mixed speech: two talker speech, male vs. female speaker (*difficult*); task: attend to pre-specified speaker
- 13 younger and 9 older listeners
- Connectivity analyzed in theta band (4-8 Hz)
- Frontal, temporal, and parietal lobes are included

NLGC captures notable network-level differences in cortex during easy and difficult listening conditions for both younger and older listeners.

Fig. 5. NLGC analysis of recorded MEG data in theta band. **A.** Extracted GC links between frontal and temporal areas overlaid on dorsal brain plots for both age groups and conditions. Notable increase of top-down links from frontal to temporal areas of younger adults as listening becomes difficult but not older. **B.** Percentage of causal links, averaged over subjects within age-group, between frontal, temporal, and parietal areas, for both conditions. Notable changes across both listening conditions and age. Frontal to temporal connections for older adults do not change significantly across listening conditions but do for younger adults. Dashed ovals indicate corresponding links in **A**.

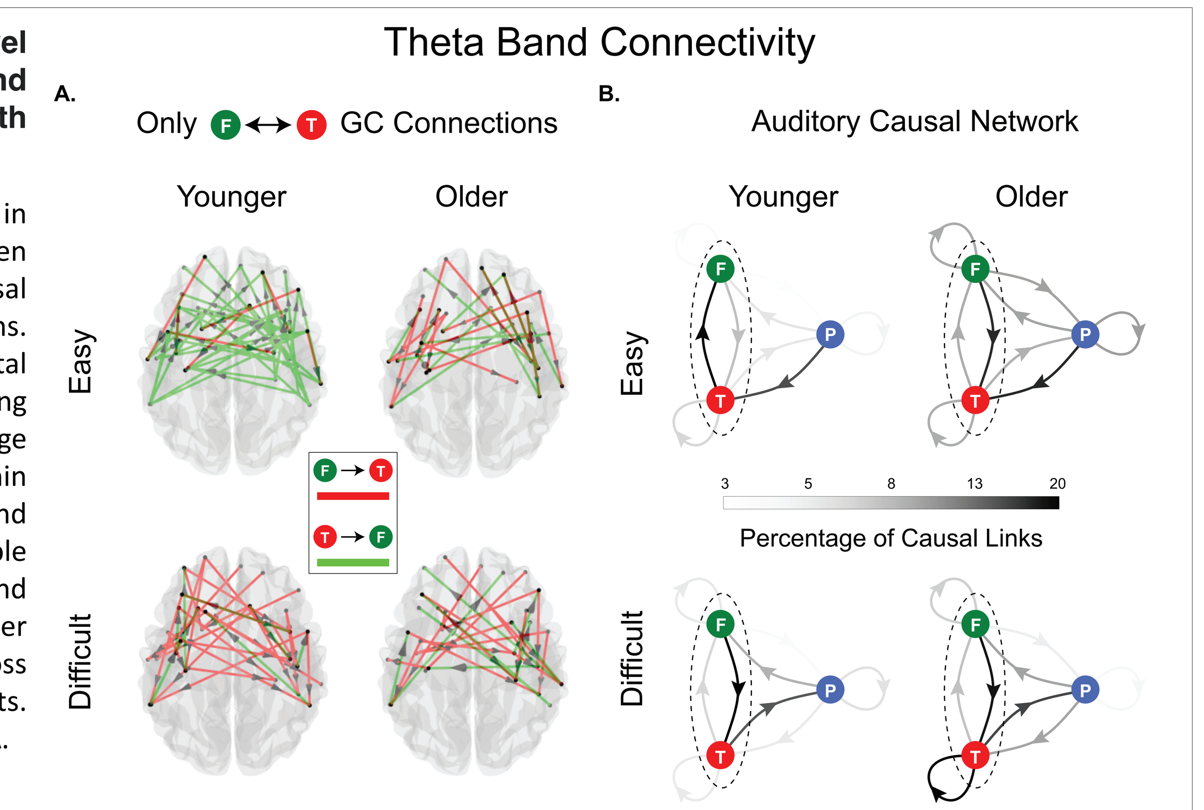

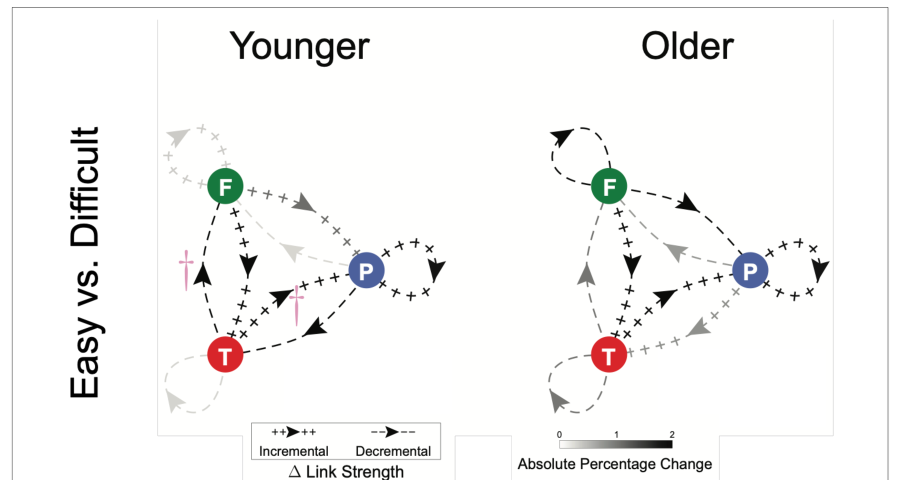

Theta-band network-level changes in cortex across *easy vs. difficult listening conditions*, for both age groups.

Fig. 6. Changes from easy to difficult condition (in percentage of causal links) averaged over subjects, between frontal, temporal, and parietal areas; all are significant. Notable (in effect-size) differences (†) by task seen in younger adults, for temporal to frontal connectivity (reduced bottom-up speech processing) and temporal to parietal (increased parietal involvement in speech processing) with task difficulty.

Theta-band network-level changes in cortex across *age groups*, for both listening conditions.

Fig. 7. Age-related changes (in percentage of causal links) averaged over subject-pairs between frontal, temporal, and parietal areas; all are significant. Notable (in effect-size) age-related difference (†) seen for easy task: less temporal to frontal connectivity, consistent with reduced bottom-up speech processing with aging.

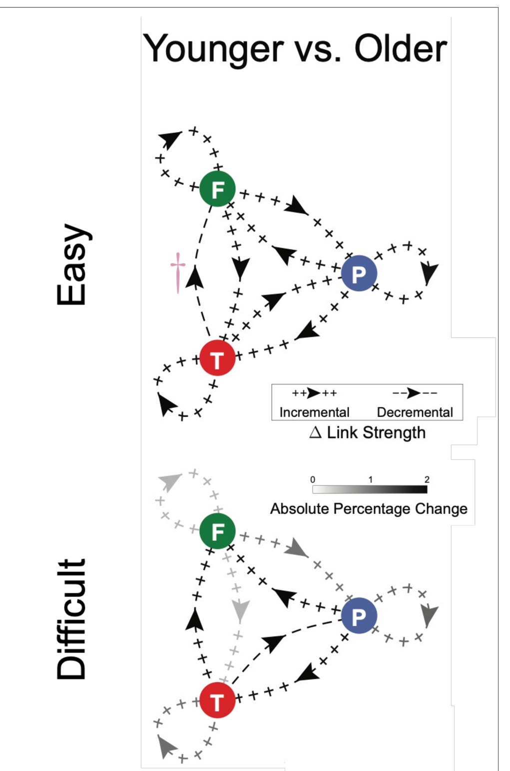

Reference

Paper:
Soleimani B, Das P, Karunathilake IMD, Kuchinsky SE, Simon JZ, Babadi B. (2022) NLGC: Network Localized Granger Causality with Application to MEG Directional Functional Connectivity Analysis, Neuroimage 260, 119496. DOI: https://doi.org/10.1016/j.neuroimage

Python Package:
Soleimani B, Das P. Network Localized Granger Causality. (2022) GitHub Repository at https://github.com/BabadiLab/NLGC

Supported by NSF (OISE 2020624, SMA 1734892 and CCF 1552946) and NIH (R01-DC019394, R01-DC014085, and P01-AG055365).